Editors' Suggestion | Featured in Physics

Low-Frequency Excess Vibrational Modes in Two-Dimensional Glasses

Lijin Wang,[1,*] Grzegorz Szamel,[2] and Elijah Flenner[2,†]

[1]School of Physics and Optoelectronics Engineering, Information Materials and Intelligent Sensing Laboratory of Anhui Province, Anhui University, Hefei 230601, People's Republic of China

[2]Department of Chemistry, Colorado State University, Fort Collins, Colorado 80523, USA

(Received 14 July 2021; accepted 9 November 2021; published 7 December 2021)

Glasses possess more low-frequency vibrational modes than predicted by Debye theory. These excess modes are crucial for the understanding of the low temperature thermal and mechanical properties of glasses, which differ from those of crystalline solids. Recent simulational studies suggest that the density of the excess modes scales with their frequency ω as ω^4 in two and higher dimensions. Here, we present extensive numerical studies of two-dimensional model glass formers over a large range of glass stabilities. We find that the density of the excess modes follows $D_{\rm exc}(\omega) \sim \omega^2$ up to around the boson peak, regardless of the glass stability. The stability dependence of the overall scale of $D_{\rm exc}(\omega)$ correlates with the stability dependence of low-frequency sound attenuation. However, we also find that, in small systems, where the first sound mode is pushed to higher frequencies, at frequencies below the first sound mode, there are excess modes with a system size independent density of states that scales as ω^3.

DOI: 10.1103/PhysRevLett.127.248001

Low-temperature glasses exhibit thermal and mechanical properties [1–7] that distinguish them from crystalline solids. The low-frequency vibrational modes in crystalline solids are plane waves. Their density of states is well described by Debye theory and scales with frequency ω as ω^{d-1} where d is the spatial dimension. For glasses, there are additional low-frequency modes that result in a peak in the reduced total density of states $D(\omega)/\omega^{d-1}$, which is referred to as the boson peak (BP) [8–11]. Understanding the nature of the additional modes provides insight into the physics behind the anomalous properties of glasses [12–20].

Mean field theory [21,22] predicts that the density of the low-frequency excess modes $D_{\rm exc}(\omega)$ grows as ω^β with $\beta = 2$, while several phenomenological models [23–27] predict $\beta = 3$ or 4. Fluctuating elasticity theory [28] predicts that $\beta = d + 1$. An analysis based on a fold stability predicts $\beta = 3$ in glasses approaching marginal stability [29], while other recent theories predict $\beta = 4$ [30–33].

Characteristics of individual modes can be examined in computer simulations, but studying finite systems presents some difficulties. One is that the plane-wave-like modes occur around discrete frequencies, which can be approximated using Debye theory. For this reason, care is needed when calculating the density of states. Simulating two-dimensional glasses adds another difficulty since Mermin-Wagner [34–37] fluctuations lead to pronounced finite size effects in some static and dynamic properties of 2D solids.

With increasing system size the glass behaves increasingly as a continuous elastic solid, and it is expected that there are plane-wave-like modes similar to those of Debye theory, which leads researchers to distinguish between plane-wave-like modes and additional modes. One simple way to do this is to use the participation ratio, which is a measure of how many particles significantly participate in the mode [38,39]. Another approach is to introduce an order parameter that quantifies the similarity between a low-frequency mode in an amorphous solid and a plane wave [39]. Although these methods are naturally suited for large systems, in principle, they can be used for systems of any size. An alternative approach is to study small systems in which the first plane-wave-like mode is pushed to higher frequencies [40]. The low-frequency modes found in these small systems are postulated to be the modes in excess of the Debye prediction.

Mizuno *et al.* [39] used the participation ratio and an order parameter to separate modes into extended and excess modes in over one-million particle, two- (2D) and three-dimensional (3D) systems. In both dimensions, they found that the density of the modes with large participation ratio obeyed Debye scaling. In 3D, they found that the density of the excess modes, which they determined are quasilocalized, scales as $D_{\rm loc}(\omega) \sim \omega^4$.

The scaling of the density of excess modes Mizuno *et al.* found in 3D agrees with the scaling observed previously by studying small systems [40]. Subsequent work by Wang *et al.* [41] confirmed the picture observed by Mizuno *et al.* in 3D in glasses of a wide range of stability. Numerical simulations have demonstrated the universality of $D(\omega) \sim \omega^4$ scaling in 3D model glass formers, irrespective of glass preparation or interaction potentials [39–54]. In their studies of large 2D systems, Mizuno *et al.* found very few low-frequency modes with small participation ratio or

with small values of plane-wave order parameter. However, Kapteijns, Bouchbinder, and Lerner [55], who studied small systems, found modes below the first plane-wave-like mode with density scaling as ω^4. The ω^4 scaling was inferred from the distribution of the minimum vibrational frequencies in Ref. [56] by studying small 2D systems. Notably, unlike in higher dimensions, Kapteijns *et al.* found that the prefactor for the ω^4 scaling grew with system size as $[\log N]^{5/2}$ in 2D. For the much larger system studied by Mizuno *et al.*, it might be expected that there would be a discernible increase in the density of states over the Debye spectrum, but the logarithmic increase with system size would make the increase modest.

In this Letter, we present results for the density of excess modes, $D_{\mathrm{exc}}(\omega)$, in 2D model glass formers with different interaction potentials and stability. We used two ways to calculate $D_{\mathrm{exc}}(\omega)$. The first method is to subtract off the Debye prediction. Except for very low frequencies, this should allow one to examine how $D_{\mathrm{exc}}(\omega)$ changes with frequency, but the discrete nature of the spectrum makes it hard to determine the low-frequency growth of $D_{\mathrm{exc}}(\omega)$. Using this procedure, we found that $D_{\mathrm{exc}}(\omega) \sim \omega^2$ in 2D. Importantly, $D_{\mathrm{exc}}(\omega)$ is correlated with the low-frequency scaling of sound attenuation, which resembles the correlation found in 3D [19]. In the second method, we studied small systems to make a more direct connection with previous results. Unlike previous work, we found a system size and model independent ω^3 scaling of the density of states far below the first mode predicted by Debye theory. However, these low-frequency modes are very rare in poorly annealed systems, and we did not find them in stable systems.

We performed extensive simulation studies of four 2D model glass formers: (I) a polydisperse system with an inverse power law potential $\propto r^{-n}$ (r is the interparticle distance) with $n = 12$ (IPL-12) [57]; (II) a bidisperse system with an inverse power law potential where $n =$ 10 (IPL-10) [44]; (III) a bidisperse system with a Lennard-Jones potential [58]; (IV) a bidisperse system with a harmonic potential [59]. Details regarding the four models can be found in the Supplemental Material [60].

We created zero-temperature glasses by instantaneously quenching equilibrated liquid configurations at parent temperatures T_p to $T = 0$ using the fast inertial relaxation engine [61]. Equilibrated liquids at high parent temperatures were obtained by performing molecular dynamic simulations using LAMMPS [62]. Glasses obtained using this method are not very stable. To generate stable glasses for the IPL-12 system, we employed the swap Monte Carlo method [63–65] to prepare equilibrated supercooled liquids at low T_p, down to $37\%T_g$, where $T_g \approx 0.082$ is the estimated experimental glass transition temperature [57].

The normal modes of $T = 0$ glasses were obtained by diagonalizing the Hessian matrix using ARPACK [66] and the Intel Math Kernel Library [67]. The density of states is given by $D(\omega) = [1/(2N - d)] \sum_{l=1}^{2N-d} \delta(\omega - \omega_l)$ with ω_l the frequency of mode l and N the number of particles. In glasses, there are no pure plane-wave modes and the frequencies of the plane-wave-like modes are clustered around the Debye predictions [68,69]. Since Debye theory predicts discrete modes in finite systems, if the bin size to be used in the calculation of $D(\omega)$ is not chosen correctly, the density is inaccurate. The calculation of the cumulative density of states $I(\omega) = \int_0^{\omega} D(\omega')d\omega'$ does not suffer from this issue since it amounts to counting the number of states up to ω and dividing by the total number of states. For this reason, we focus on $I(\omega)$.

To obtain the excess modes, Mizuno and coworkers [39] defined a threshold of the participation ratio $P_c = 0.01$ to divide plane-wave-like modes and quasilocalized modes. They concluded that there are few to no low-frequency quasilocalized modes in poorly annealed 2D glasses [39]. Additionally, the Debye theory accurately predicted the low-frequency density of states, but there was still a boson peak at higher frequencies. We attempted to use the participation ratio to separate the modes, but we found that the scaling behavior of the excess modes in 2D stable IPL-12 model glasses depends strongly on P_c, which makes it impossible to determine the scaling of $I(\omega)$ using the participation ratio. Therefore, we utilized a different procedure by subtracting from $I(\omega)$ the Debye prediction [28]

$$I_{\mathrm{exc}}(\omega) = I(\omega) - I_D(\omega), \tag{1}$$

where $I_D(\omega)$ is the Debye prediction [70], $I_D(\omega) = A_D\omega^d/d$ with Debye level A_D determined from mechanical moduli [70]. This procedure does not take into account that the mode frequencies are discrete for finite systems.

Figure 1(a) shows $I_{\mathrm{exc}}(\omega)$ for our 2D IPL-12 model glasses for $N = 20\,000$ at different parent temperatures T_p. The glass's stability increases with decreasing T_p [41,47,57]. We use parent temperatures ranging from $T_p = 0.400$, which is above the onset temperature of slow dynamics $T_o = 0.250$, down to $T_p = 0.030$, which is below $T_g = 0.082$ [57]. For the lowest frequencies where we can clearly estimate a power law, we find that $I_{\mathrm{exc}}(\omega) \simeq A_2\omega^3/3$, which suggests that $D_{\mathrm{exc}}(\omega) \simeq A_2\omega^2$. We find that this scaling continues to about the Ioffe-Regel limit or the boson peak frequency [10], irrespective of the glass's stability. We find that the coefficient quantifying the magnitude of the excess modes density, A_2, is stability dependent, Fig. 1(b). A_2 decreases by a factor of 13 for our lowest T_p. This indicates that there are fewer excess modes for increasingly stable 2D glasses, which is consistent with observations for 3D glasses [41,47,54].

Previous work [18,19,28] found a connection between sound attenuation and density of excess low-frequency modes. In particular, in Ref. [19], we showed that the

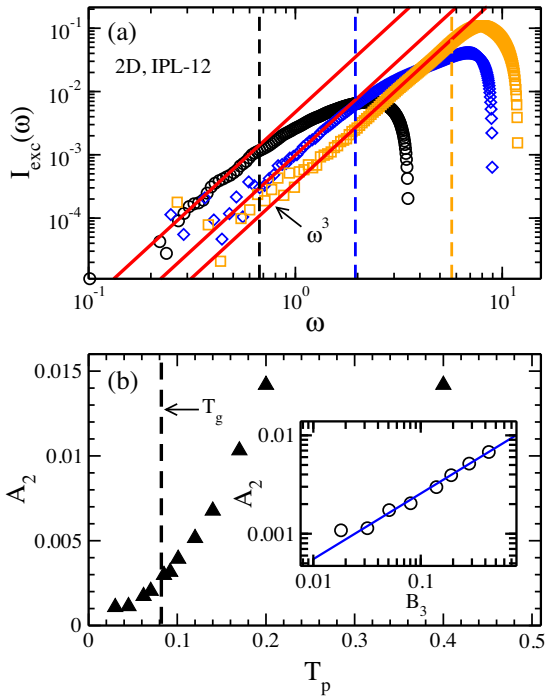

FIG. 1. (a) Cumulative density of states of excess modes $I_{\rm exc}(\omega) = I(\omega) - I_D(\omega)$ at $T_p = 0.400$ (circles), 0.085 (diamonds), and 0.030 (squares) in $N = 20\,000$ system in the 2D IPL-12 model. $I(\omega)$ is the total cumulative density of states while $I_D(\omega) = A_D\omega^2/2$. The red lines are fits to $I_{\rm exc}(\omega) = A_2\omega^3/3$ while vertical lines indicate boson peak frequencies. (b) T_p dependence of A_2, with the estimated glass transition temperature T_g indicated for reference. Glass stability increases with decreasing T_p. (Inset) A_2 against the prefactor B_3 in $\Gamma(\omega) = B_3\omega^3$ with Γ the transverse sound attenuation coefficient. Details for the calculation of Γ can be found in Ref. [19]. The blue line indicates a fit to $A_2 \sim B_3^{\gamma}$ with $\gamma \approx 2/3$.

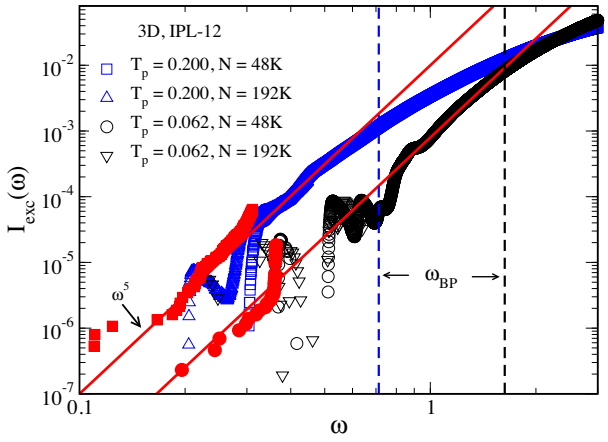

FIG. 2. Cumulative density of states of excess modes $I_{\rm exc}(\omega) = I(\omega) - I_D(\omega)$ in the 3D IPL-12 model glasses, with the boson peak frequency $\omega_{\rm BP}$ indicated. $I(\omega)$ is the total cumulative density of states and $I_D(\omega) = A_D\omega^3/3$. Red filled squares and circles represent $I(\omega)$ at frequencies below around the first Debye frequency at $T_p = 0.200$ and $T_p = 0.062$, respectively, in the $N = 48\,000$ system. The red lines correspond to $I_{\rm exc}(\omega) \sim \omega^5$.

prefactor B_4 in the sound attenuation coefficient $\Gamma(\omega) = B_4\omega^4$ scales linearly with the prefactor A_4 in the scaling $I_{\rm exc}(\omega) = A_4\omega^5/5$ in 3D glasses. Inspired by this result, we examined whether A_2 is related to the prefactor B_3 in the sound attenuation coefficient $\Gamma(\omega) = B_3\omega^3$ in 2D. Previously, B_3 was found to decrease with increasing glass stability [18]. Here, we find $A_2 \sim B_3^{\gamma}$ with $\gamma \approx 2/3$, and thus, we establish that, in 2D, the density of the excess modes is related to sound attenuation, which is consistent with our result for 3D glasses [19]. Further work is needed to elucidate the nonlinear relationship between A_2 and B_3 in 2D, which contrasts with $A_4 \propto B_4$ in 3D.

Since the method introduced here is different from methods used before, we checked what results it produces for 3D glasses where it has been firmly established that $I_{\rm exc}(\omega) \sim \omega^5$. In Fig. 2, we show $I_{\rm exc}(\omega)$ in 3D IPL-12 glasses for two stabilities, a poorly annealed glass with $T_p = 0.200$ and a stable glass with $T_p = 0.062$ (the same glasses were examined in Ref. [41]). We find that $I_{\rm exc}(\omega) \sim \omega^5$ up to a frequency close to the boson peak for both glasses, which indicates the resulting scaling of $I_{\rm exc}(\omega)$ determined using Eq. (1) is consistent with that of $I_{\rm exc}(\omega)$ calculated with previously used procedures [39,41,43]. Additionally, these results suggest that, in 3D, the end of the ω^5 scaling of $I_{\rm exc}(\omega)$ is around the boson peak frequency. We note that our procedure cannot be used for frequencies below the lowest plane wave mode frequency. More importantly, it will only reveal the proper scaling if there is a near continuum of modes [68].

It has been claimed [40,48,55] that the scaling of the excess modes could be obtained from the low-frequency density of states for small systems since the frequency of the lowest plane-wave-like mode is pushed up. One may expect the total cumulative density of states $I(\omega) = I_{\rm exc}(\omega)$ for low frequencies if the excess modes were independent of the plane-wave-like modes, which we found for 3D glasses with different stabilities, see Fig. 2. The low-frequency tail of $I(\omega)$ is well described by a power law $I_{\rm exc}(\omega) \sim \omega^5$ for $T_p = 0.200$ and $T_p = 0.062$. However, in 2D glasses much below the first Debye frequency, we find $I(\omega) \sim \omega^4$, which suggests that $D(\omega) \sim \omega^3$. Previous studies reported $D(\omega) \sim \omega^4$ in 2D [55,56], which would imply that $I(\omega) \sim \omega^5$. To make sure this observation is model independent, we repeated this procedure for different model glass formers.

In Fig. 3, we show $I(\omega)$ for $N = 3000$ system in the 2D IPL-12 model. There is a range of frequencies below the lowest Debye mode frequency ($\approx$0.261) where $I(\omega) \sim \omega^4$. To check this scaling, we examined $I(\omega)/\omega^4$, see the inset to Fig. 3, and we found that there is a low-frequency plateau. Previous results suggest that $I(\omega) \sim \omega^5$ at frequencies much below the first Debye mode in 2D glasses [55,56]. However, we find that the ω^5 scaling is only valid

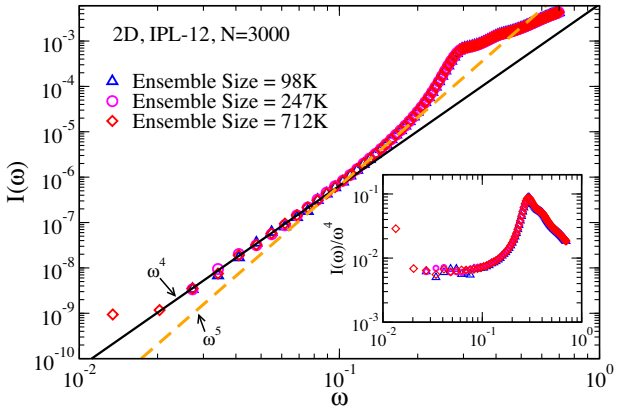

FIG. 3. The total cumulative density of states $I(\omega)$ for $N = 3000$ system at $T_p = 0.400$ with different ensemble sizes N_{En} in the 2D IPL-12 model. The solid and dashed lines represent power laws of ω^4 and ω^5, respectively, while the dash-dotted line indicates Debye scaling $I(\omega) = A_D\omega^2/2$. For reference, the lowest Debye mode frequency is about 0.261. (Inset) The same data plotted as $I(\omega)/\omega^4$ vs ω.

for an intermediate-frequency regime below the peak of $I(\omega)$ and appears to be a transient between the low-frequency scaling and the change of the scaling due to the emergence of plane-wave-like modes.

Moreover, we found that this low-frequency $I(\omega) \sim \omega^4$ scaling in 2D does not depend on the model glass former, see Fig. 1 of the Supplemental Material [60]. There are common features shared by each model. First, the prefactor of the scaling law does not depend on system size. This conclusion is different than the conclusion of Ref. [55] that $I(\omega) = A_4\omega^5/5$ and the prefactor A_4 grows as $(\log N)^{5/2}$. Second, the quartic law works up to a larger frequency with decreasing system size.

There are very few modes that contribute to the low-frequency ω^4 scaling of $I(\omega)$ for our least stable 2D glass. On average, there is only one mode in the low-frequency $I(\omega) \sim \omega^4$ regime every one hundred configurations for the $N = 3000$ system. The lower the frequency we want to examine, the larger the ensemble size N_{En} (number of configurations) we need. However, we do not observe N_{En} dependence of the $I(\omega) \sim \omega^4$ regime in $N = 3000$ system when N_{En} ranges from around 100 000 to 710 000, see Fig. 3. The same conclusion can also be drawn in our study of the $N = 1000$ system where N_{En} is around 2 200 000 [60]. We checked that the previously reported ω^5 scaling in some systems is due to ensemble size not being large enough, which hinders the observation of the ω^4 scaling at much lower frequencies. We also find that the ω^5 scaling regime vanishes for very small systems [60]. Since the number of these low-frequency modes decreases with increasing stability, we could not examine the stability dependence of these modes. We do not exclude the possibility that annealing can change the scaling of $I(\omega)$ [45,53].

In conclusion, we utilized two methods to examine the excess density of states in 2D glasses. In large systems, we found evidence that the excess density of states scales as $A_2\omega^2$, and A_2 correlates with the sound attenuation coefficient. However, in small systems, we found that the modes below the lowest Debye frequency have density of states scaling as ω^3, with a system-size independent prefactor. This inconsistent behavior is not found in 3D glasses.

Our results leave several open questions. First, why is the scaling of excess modes different above and below the lowest Debye frequency? One possibility is that our systems are not large enough to accurately determine $I_{\mathrm{exc}}(\omega)$ by subtracting off the Debye contribution at low frequencies. However, we do find a frequency range where the excess density of states calculated by subtracting off the Debye contribution exhibits systematic deviation from the density of excess states in small systems, see Fig. 4 of the Supplemental Material [60]. Thus, it seems that the presence of plane waves influences the behaviors of the excess density of states in 2D glasses.

Second, is it possible that the ω^2 and ω^3 scalings do not extend to $\omega = 0$? A gap in the excess density of states would be consistent with the conclusions of Ref. [39]. It is very difficult to numerically test this since the ω^2 and ω^3 scalings represent very few modes. Future theoretical work may shed some light on this issue.

Third, why is the excess density of states of 2D glasses different from that of 3D glasses? Fluctuating elasticity theory predicts that $D_{\mathrm{exc}}(\omega)$ depends on spatial dimension as ω^{d+1} [28]. Thus, the predicted $D_{\mathrm{exc}}(\omega) \sim \omega^4$ in 3D glasses is consistent with 3D numerical observations. The predicted scaling of $D_{\mathrm{exc}}(\omega) \sim \omega^3$ of 2D glasses is consistent with what we find in small systems.

Finally, is it possible that the upper frequency cutoff of the low-frequency scaling, ω_g, is below the frequency range where we found ω^2 scaling of $D_{\mathrm{exc}}(\omega)$ in large 2D glasses? If this were the case, it would differ from our finding in 3D that ω_g is around the boson peak frequency. Future work should examine what determines ω_g and its d dependence.

The dimensional dependence of properties of glasses has implications of the nature of the glass transition and the theoretical understanding of the properties of glasses. This work is another demonstration that some characteristics of 2D and 3D glasses profoundly differ, and thus, any extrapolation of the properties of two-dimensional glasses to higher dimensions should be done with care.

We wish to thank Andrea Ninarello for generously providing equilibrated configurations at very low parent temperatures and E. Lerner for comments on the manuscript. L. W. acknowledges support from National Natural Science Foundation of China (Grant No. 12004001), Anhui Province (Grant No. S020218016), Hefei City (Grant No. Z020132009), and Anhui University (Start-up fund).

E. F. and G. S. acknowledge support from NSF Grant No. CHE-1800282. We also acknowledge Beijing Super Cloud Computing Center, the High-Performance Computing Platform of Anhui University, and Beijing Computational Science Research Center for providing computing resources.

*lijin.wang@ahu.edu.cn
†flennere@gmail.com

[1] R. C. Zeller and R. O. Pohl, Phys. Rev. B **4**, 2029 (1971).
[2] P. W. Anderson, B. I. Halperin, and C. M. Varma, Philos. Mag. **25**, 1 (1972).
[3] W. A. Phillips, J. Low Temp. Phys. **7**, 351 (1972).
[4] M. P. Zaitlin and A. C. Anderson, Phys. Rev. B **12**, 4475 (1975).
[5] R. O. Pohl, X. Liu, and E. Thompson, Rev. Mod. Phys. **74**, 991 (2002).
[6] M. Ozawa, L. Berthier, G. Biroli, A. Rosso, and G. Tarjus, Proc. Natl. Acad. Sci. U.S.A. **115**, 6656 (2018).
[7] J. Ketkaew, W. Chen, H. Wang, A. Datye, M. Fan, G. Pereira, U. D. Schwarz, Z. Liu, R. Yamada, W. Dmowski, M. D. Shattuck, C. S. O'Hern, T. Egami, E. Bouchbinder, and J. Schroers, Nat. Commun. **9**, 3271 (2018).
[8] T. S. Grigera, V. Martin-Mayor, G. Parisi, and P. Verrocchio, Nature (London) **422**, 289 (2003).
[9] K. Inoue, T. Kanaya, S. Ikeda, K. Kaji, K. Shibata, M. Misawa, and Y. Kiyanagi, J. Chem. Phys. **95**, 5332 (1991).
[10] H. Shintani and H. Tanaka, Nat. Mater. **7**, 870 (2008).
[11] U. Buchenau, A. Wischnewski, M. Ohl, and E. Fabiani, J. Phys. Condens. Matter **19**, 205106 (2007).
[12] K. Chen, M. L. Manning, P. J. Yunker, W. G. Ellenbroek, Z. X. Zhang, A. J. Liu, and A. G. Yodh, Phys. Rev. Lett. **107**, 108301 (2011).
[13] A. Widmer-Cooper, H. Perry, P. Harrowell, and D. R. Reichman, Nat. Phys. **4**, 711 (2008).
[14] S. S. Schoenholz, A. J. Liu, R. A. Riggleman, and J. Rottler, Phys. Rev. X **4**, 031014 (2014).
[15] M. L. Manning and A. J. Liu, Phys. Rev. Lett. **107**, 108302 (2011).
[16] J. Zylberg, E. Lerner, E. Y. Bar-Sinai, and E. Bouchbinder, Proc. Natl. Acad. Sci. U.S.A. **114**, 7289 (2017).
[17] E. Flenner, L. Wang, and G. Szamel, Soft Matter **16**, 775 (2020).
[18] A. Moriel, G. Kapteijns, C. Rainone, J. Zylberg, E. Lerner, and E. Bouchbinder, J. Chem. Phys. **151**, 104503 (2019).
[19] L. Wang, L. Berthier, E. Flenner, P. Guan, and G. Szamel, Soft Matter **15**, 7018 (2019).
[20] N. Xu, V. Vitelli, A. J. Liu, and S. R. Nagel, Europhys. Lett. **90**, 56001 (2010).
[21] E. DeGiuli, A. Laversanne-Finot, G. Düring, E. Lerner, and M. Wyart, Soft Matter **10**, 5628 (2014).
[22] S. Franz, G. Parisi, P. Urbani, and F. Zamponi, Proc. Natl. Acad. Sci. U.S.A. **112**, 14539 (2015).
[23] U. Buchenau, Yu. M. Galperin, V. L. Gurevich, and H. R. Schober, Phys. Rev. B **43**, 5039 (1991).
[24] H. R. Schober and C. Oligschleger, Phys. Rev. B **53**, 11469 (1996).
[25] V. L. Gurevich, D. A. Parshin, and H. R. Schober, Phys. Rev. B **67**, 094203 (2003).
[26] V. Gurarie and J. T. Chalker, Phys. Rev. B **68**, 134207 (2003).
[27] A. Kumar, I. Procaccia, and M. Singh, arXiv:2102.12368.
[28] W. Schirmacher, G. Ruocco, and T. Scopigno, Phys. Rev. Lett. **98**, 025501 (2007).
[29] N. Xu, A. J. Liu, and S. R. Nagel, Phys. Rev. Lett. **119**, 215502 (2017).
[30] H. Ikeda, Phys. Rev. E **99**, 050901(R) (2019).
[31] E. Stanifer, P. K. Morse, A. A. Middleton, and M. L. Manning, Phys. Rev. E **98**, 042908 (2018).
[32] E. Bouchbinder, E. Lerner, C. Rainone, P. Urbani, and F. Zamponi, Phys. Rev. B **103**, 174202 (2021).
[33] W. Ji, M. Popović, T. W. J. de Geus, E. Lerner, and M. Wyart, Phys. Rev. E **99**, 023003 (2019).
[34] E. Flenner and G. Szamel, Nat. Commun. **6**, 7392 (2015).
[35] S. Vivek, C. P. Kelleher, P. M. Chaikin, and E. R. Weeks, Proc. Natl. Acad. Sci. U.S.A. **114**, 1850 (2017).
[36] B. Illing, S. Fritschi, H. Kaiser, C. L. Klix, G. Maret, and P. Keim, Proc. Natl. Acad. Sci. U.S.A. **114**, 1856 (2017).
[37] E. Flenner and G. Szamel, Proc. Natl. Acad. Sci. U.S.A. **116**, 2015 (2019).
[38] V. Mazzacurati, G. Ruocco, and M. Sampoli, Europhys. Lett. **34**, 681 (1996).
[39] H. Mizuno, H. Shiba, and A. Ikeda, Proc. Natl. Acad. Sci. U.S.A. **114**, E9767 (2017).
[40] E. Lerner, G. Düring, and E. Bouchbinder, Phys. Rev. Lett. **117**, 035501 (2016).
[41] L. Wang, A. Ninarello, P. Guan, L. Berthier, G. Szamel, and E. Flenner, Nat. Commun. **10**, 26 (2019).
[42] M. Baity-Jesi, V. Martin-Mayor, G. Parisi, and S. Perez-Gaviro, Phys. Rev. Lett. **115**, 267205 (2015).
[43] M. Shimada, H. Mizuno, and A. Ikeda, Phys. Rev. E **97**, 022609 (2018).
[44] G. Kapteijns, E. Bouchbinder, and E. Lerner, J. Chem. Phys. **148**, 214502 (2018).
[45] E. Lerner, Phys. Rev. E **101**, 032120 (2020).
[46] L. Angelani, M. Paoluzzi, G. Parisi, and G. Ruocco, Proc. Natl. Acad. Sci. U.S.A. **115**, 8700 (2018).
[47] C. Rainone, E. Bouchbinder, and E. Lerner, Proc. Natl. Acad. Sci. U.S.A. **117**, 5228 (2020).
[48] S. Bonfanti, R. Guerra, C. Mondal, I. Procaccia, and S. Zapperi, Phys. Rev. Lett. **125**, 085501 (2020).
[49] D. Richard, K. González-López, G. Kapteijns, R. Pater, T. Vaknin, E. Bouchbinder, and E. Lerner, Phys. Rev. Lett. **125**, 085502 (2020).
[50] M. Shimada, H. Mizuno, L. Berthier, and A. Ikeda, Phys. Rev. E **101**, 052906 (2020).
[51] P. Das and I. Procaccia, Phys. Rev. Lett. **126**, 085502 (2021).
[52] M. Shimada, H. Mizuno, M. Wyart, and A. Ikeda, Phys. Rev. E **98**, 060901(R) (2018).
[53] E. Lerner and E. Bouchbinder, Phys. Rev. E **96**, 020104(R) (2017).
[54] W. Ji, T. W. J. de Geus, M. Popović, E. Agoritsas, and M. Wyart, Phys. Rev. E **102**, 062110 (2020).
[55] G. Kapteijns, E. Bouchbinder, and E. Lerner, Phys. Rev. Lett. **121**, 055501 (2018).

[56] V. V. Krishnan, K. Ramola, and S. Karmakar, arXiv:2104.09181.
[57] L. Berthier, P. Charbonneau, A. Ninarello, M. Ozawa, and S. Yaida, Nat. Commun. **10**, 1508 (2019).
[58] R. Bruning, D. A. St-Onge, S. Patterson, and W. Kob, J. Phys. Condens. Matter **21**, 035117 (2009).
[59] C. S. O'Hern, L. E. Silbert, A. J. Liu, and S. R. Nagel, Phys. Rev. E **68**, 011306 (2003).
[60] See Supplemental Material at http://link.aps.org/supplemental/10.1103/PhysRevLett.127.248001 for simulation details of the four interaction potential models and more supporting analysis.
[61] E. Bitzek, P. Koskinen, F. Gähler, M. Moseler, and P. Gumbsch, Phys. Rev. Lett. **97**, 170201 (2006).
[62] S. Plimpton, J. Comput. Phys. **117**, 1 (1995).
[63] T. S. Grigera and G. Parisi, Phys. Rev. E **63**, 045102(R) (2001).
[64] A. Ninarello, L. Berthier, and D. Coslovich, Phys. Rev. X **7**, 021039 (2017).
[65] L. Berthier, D. Coslovich, A. Ninarello, and M. Ozawa, Phys. Rev. Lett. **116**, 238002 (2016).
[66] http://www.caam.rice.edu/software/ARPACK/.
[67] https://software.intel.com/en-us/mkl/.
[68] E. Bouchbinder and E. Lerner, New J. Phys. **20**, 073022 (2018).
[69] G. Kapteijns, E. Bouchbinder, and E. Lerner, Phys. Rev. E **104**, 035001 (2021).
[70] C. Kittel, *Introduction to Solid State Physics*, 7th ed. (Wiley, New York, 1996).